

# Exotic Photon Searches at CDF II

Eunsin Lee (for the CDF Collaboration)

Department of Physics, Texas A&M University, College Station, TX 77843, USA

We present recent results of searches for exotic photons at CDF II. In the first signature-based search, we search for anomalous production of two photons with additional energetic objects. The results are consistent with the standard model expectations. In the second analysis, we present a signature-based search for anomalous production of events containing a photon, two jets, of which at least one is identified as originating from a  $b$  quark, and missing transverse energy. We find no indications of non-standard model phenomena. Finally, a search for a fermiophobic Higgs in the diphoton final state is presented. Since no evidence of a resonance in the diphoton mass spectrum is observed we exclude this Higgs boson with mass below  $106 \text{ GeV}/c^2$  at a 95% confidence level.

## 1. Introduction

Over the last decades, the fast developments in phenomenology and model-building have high-energy physicists at the Tevatron with a number of new physics scenarios to investigate. Searches at CDF have been either broad signature-based searches in accessible data samples for any discrepancy with the standard model (SM) in event yields or a specific new physics model-based searches. The signature-based searches proceed quickly in unprejudiced way as well as cover many new physics models. The model-based searches are highly sensitive for a particular model, and provide limits on the model. In this report we present two results using the signature-based search approach and one result in a model-based approach. All of these analyses use photons in the final state.

## 2. Search for Anomalous Production of

$\gamma\gamma + X$

We define a “baseline” sample with two isolated, central ( $0.05 < |\eta| < 1.05$ ) photons with  $E_T > 13 \text{ GeV}$ . We then select subsamples which also contain at least one more energetic, isolated and well-defined object or where two photons are accompanied by large missing transverse energy ( $\cancel{E}_T$ ). The additional object may be an electron ( $e$ ), muon ( $\mu$ ),  $\tau$ -lepton ( $\tau$ ), or jets. The integrated luminosity for each subsample varies from 1 to  $2 \text{ fb}^{-1}$ . In next subsections we address each  $\gamma\gamma + X$  ( $X = e/\mu, \tau$  and  $\cancel{E}_T$ ) subsample in turn. We describe the definition of the subsamples, the calculation of the SM predictions, and the comparison of the data and the predictions. Unless it is otherwise noted, all analyses use the same definitions of the additional objects and kinematic variables: electrons, muons,  $\tau$ -leptons, jets, soft unclustered energy,  $\cancel{E}_T$ , and  $H_T$ . The  $H_T$  is defined as a scalar sum of  $\cancel{E}_T$  and  $E_T$ 's of all identified photons, leptons, and jets.

### 2.1. The $\gamma\gamma + e/\mu$ Final State

We search in  $1.1 \text{ fb}^{-1}$  of data for anomalous production of events containing two photons and at least one additional electron or muon. The selected  $\gamma\gamma e$  and  $\gamma\gamma\mu$  events must have at least one electron (central or forward) or muon ( $|\eta| < 1.0$ ) candidate with  $E_T^e > 20 \text{ GeV}$  and  $p_T^\mu > 20 \text{ GeV}/c$ , respectively. Backgrounds for the  $\gamma\gamma e$  and  $\gamma\gamma\mu$  signatures of new physics include the SM production of  $Z \rightarrow l^+l^-$  and  $W \rightarrow l\bar{\nu}_l$  in association with two photons ( $Z\gamma\gamma$ ,  $W\gamma\gamma$ ), where photons are radiated from either the initial state quarks, charged electroweak boson ( $W$ ), or the final-state leptons. Also there are misidentification backgrounds (fake photons or leptons). Backgrounds for the  $\gamma\gamma e$  channel is dominated by  $Z\gamma$  production with an electron being misidentified as a photon. This is estimated by defining a sample of events with two electrons and one photon, then applying a probability, which is derived in data, for an electron to be misidentified as a photon. We find three  $\gamma\gamma e$  events with an expected SM backgrounds of  $6.82 \pm 0.75$ . In the  $\gamma\gamma\mu$  channel the leading background is the electroweak tri-boson production of  $Z\gamma\gamma$ . We find no  $\gamma\gamma\mu$  events and expect  $0.79 \pm 0.11$  events. Figure 1 shows the  $H_T$  distributions from data and the predicted backgrounds and we do not see any evidence for anomalous production of  $\gamma\gamma e$  and  $\gamma\gamma\mu$  events.

### 2.2. The $\gamma\gamma + \tau$ Final State

We search for  $2.0 \text{ fb}^{-1}$  of data for events with two photons and a hadronically decaying  $\tau$ -lepton. The selected  $\gamma\gamma\tau$  events must have at least one  $\tau$ -lepton candidate identified using the tight requirements and passing  $E_T > 15 \text{ GeV}$ . We consider two sources of backgrounds: the SM production of  $W \rightarrow \tau\nu$  or  $Z \rightarrow \tau\tau$  with photons and  $\gamma\gamma$  events with jets misidentified as  $\tau$ -leptons. The dominant background in this search is from  $\gamma\gamma + jets$  events where one of the jets is misidentified as a  $\tau$ -lepton. To estimate this background, we select events with two photons and a “loose”  $\tau$ -lepton candidate and apply the  $jet \rightarrow \tau$

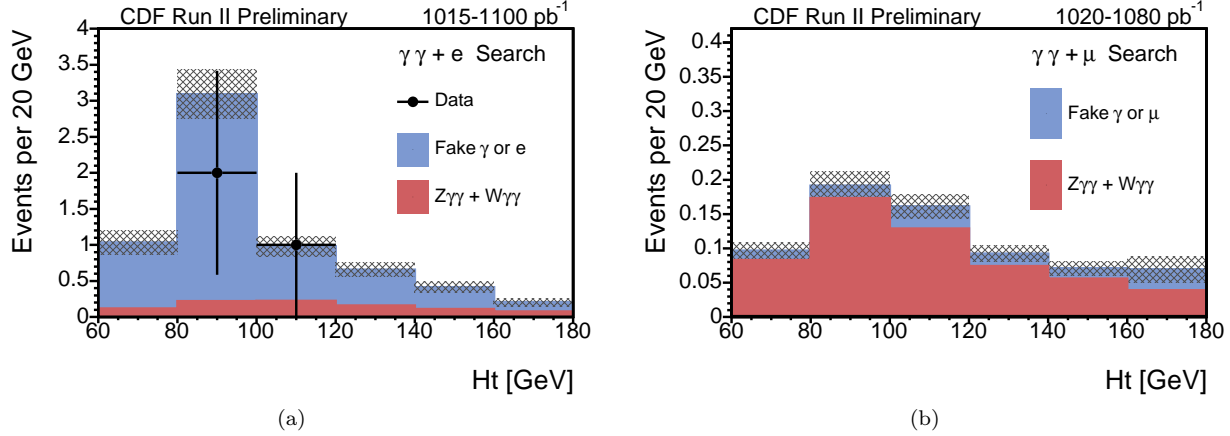


Figure 1: In (a) the  $H_T$  distributions of the  $\gamma\gamma e$  events from the SM prediction and the three events observed in the data. In (b) the  $H_T$  distributions of the  $\gamma\gamma\mu$  events with zero observed events.

misidentification probability. Since the misidentification probability is different for jets originated by quarks or by gluons, and the ratio of quark jets to gluon jets may be different than in the sample used to derive the  $jet \rightarrow \tau$  misidentification probability, we corrected for this effect. We observe 34 events with  $46 \pm 10$  expectation. Figure 2 also shows the  $H_T$  distribution for the selected  $\gamma\gamma + \tau$  candidate events and the predicted SM background, which indicates there is no anomalies.

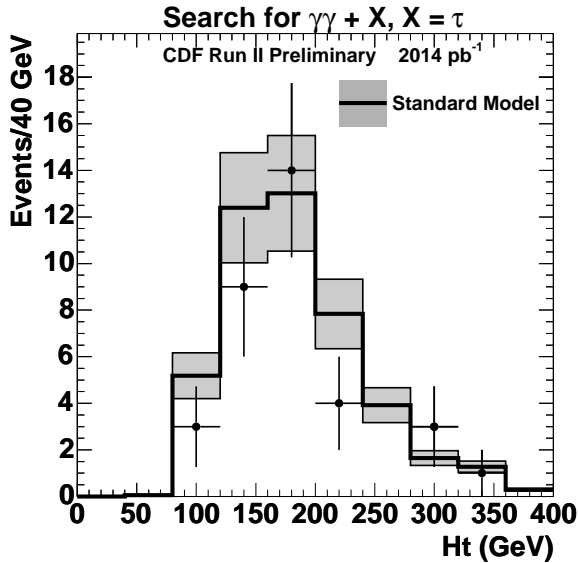


Figure 2: The  $H_T$  distribution in  $\gamma\gamma + \tau$  candidate events and the SM backgrounds.

### 2.3. The $\gamma\gamma + \cancel{E}_T$ Final State

We search for the anomalous production of two photons and large missing transverse energy ( $\cancel{E}_T$ ) in 2 fb<sup>-1</sup> of data. The  $\cancel{E}_T$  is defined as an energy imbalance in the calorimeter and is an experimental signature of neutrino or new weakly interacting particle. The  $\cancel{E}_T$ , however, can be mimicked by a simple energy misreconstruction in SM events ("fake"  $\cancel{E}_T$ ): for example, fluctuations in jet energy measurements. A better separation between events with real and fake  $\cancel{E}_T$  can be achieved if a significance of the measured  $\cancel{E}_T$  is considered rather than its absolute value. The  $\cancel{E}_T$ -significance is a dimensionless quantity based on the energy resolution of jets and soft unclustered energy, taking into account the event topology. As shown in Fig. 3, the  $\cancel{E}_T$ -significance distributions have very different shapes in events with fake and real  $\cancel{E}_T$ : exponentially falling (solid line) and almost flat shapes, respectively. Thus, the  $\cancel{E}_T$ -significance is an efficient tool in separating such events. For example, a cut on the  $\cancel{E}_T$ -significance > 5 which reduces the mismeasured-energy background by a factor of  $10^5$ , the sample becomes dominated by  $W\gamma$  production, where the electron is misidentified as a photon. This background is estimated from Monte Carlo (MC) normalized to data. We observed 23 events and an expectation of  $27.3 \pm 2.3$  events.

We have also re-optimized the sample for the GMSB model [1]. In this model, all SUSY pair production decays to two neutralinos, the next-to-lightest SUSY particle, each of which then decays to a photon and a gravitino, the lightest SUSY particle ( $\tilde{\chi}_1^0 \rightarrow \gamma\tilde{G}$ ). We thus have two photons,  $\cancel{E}_T$ , and other high- $E_T$  objects in the final state. Using optimal set of cuts ( $\cancel{E}_T$ -significance,  $H_T$ , and  $\Delta\phi(\gamma_1, \gamma_2)$  between two photons) we set the world's best limit on the  $\tilde{\chi}_1^0$  mass of 149 GeV/c<sup>2</sup> at lifetime below 1 ns. The results are shown in Fig. 4.

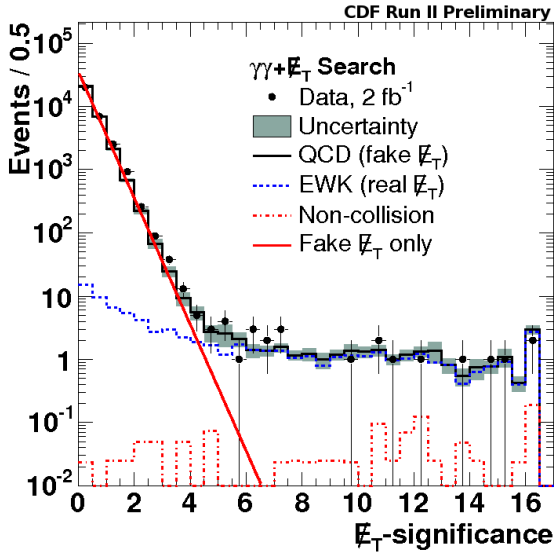


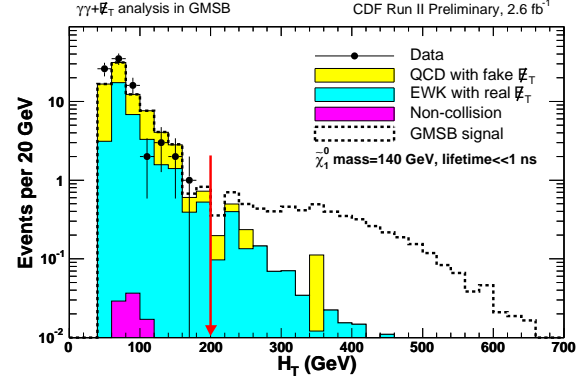
Figure 3: The  $E_T$ -significance distribution in all  $\gamma\gamma$  candidate events from the baseline sample. The QCD backgrounds with fake  $E_T$  are well separated from the EWK backgrounds with real  $E_T$ .

### 3. Search for Anomalous Production of Events with $\gamma$ , jet, $b$ -quark jet, and $E_T$

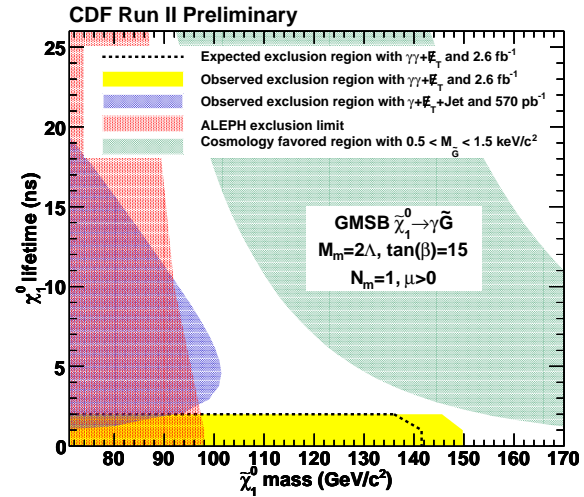
We search for new physics in the inclusive  $\gamma b j E_T$  channel using  $2.0 \text{ fb}^{-1}$  of data. We select an enhanced sample of events collected by an inclusive isolated photon trigger. We require a central ( $|\eta| < 1.1$ ) photon with  $E_T > 25 \text{ GeV}$ , two jets with  $|\eta| < 2.0$  and  $E_T > 15 \text{ GeV}$ , at least one of which is identified as originating from a  $b$ -quark ( $b$ -tagged), and  $E_T$  greater than  $25 \text{ GeV}$ .

The backgrounds are misidentified photons (“misidentified  $\gamma$ ”), true photon plus light quark jet misidentified as heavy flavor (“true  $\gamma$ , misidentified  $b$ ”), true photon plus true  $b$ -tagged jet (“ $\gamma b$ ”), and true photon plus  $c$ -quark jet (“ $\gamma c$ ”). The misidentified  $\gamma$  background is estimated from the data sample by using cluster-shape variables from the CES and hit rates in the CPR (the CES/CPR method). This technique allows the determination of the number of photon candidates in the sample that are actually misidentified jets as well as the corresponding shapes of the distributions of kinematic variables.

The true  $\gamma$ , misidentified  $b$  background is estimated by first selecting events we then apply the true-photon weight (the probability that a photon candidate is a photon) determined using the CES/CPR method and the heavy-flavor mistag rate. Because the CES/CPR method and the mistag parameterization provide event-by-event weights, we are able to determine the shapes of kinematic distributions as well as the number of events for this background.



(a)



(b)

Figure 4: The N-1 predicted kinematic distribution along with data after the optimized requirements are shown in Figure (b). There is no evidence for new physics and the data is well modeled by backgrounds alone. In (b) the predicted and observed exclusion region along with the limit from ALEPH/LEP [2] and the  $\gamma + E_T + \text{jet}$  delayed photon analysis [3]. We have a mass reach of  $141 \text{ GeV}/c^2$  (predicted) and  $149 \text{ GeV}/c^2$  (observed) at the lifetime up to 1 ns. The green shaded band shows the parameter space where  $0.5 < m_{\tilde{\chi}_1^0} < 1.5 \text{ keV}/c^2$ , favored in cosmologically consistent models [4].

We estimate the  $\gamma b$  and  $\gamma c$  backgrounds by generating MC events. We obtain the overall normalizations of these backgrounds by fitting the secondary vertex mass distribution of the tagged jets,  $m(SV)$ , to templates built from the mass distributions of the expected SM components. We first subtract the contribution due to misidentified photons by applying the CES/CPR method to obtain the number of misidentified photon events. We then estimate the fraction of heavy flavor in events with a misidentified photon by fitting the secondary vertex mass distribution in a sample enriched with jets faking photons. We then

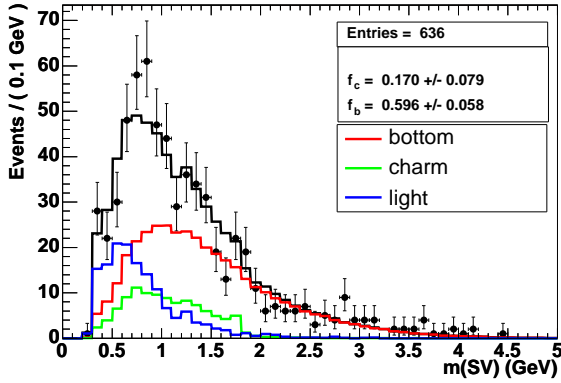


Figure 5: The secondary vertex mass fit in events containing standard photons for the search sample.

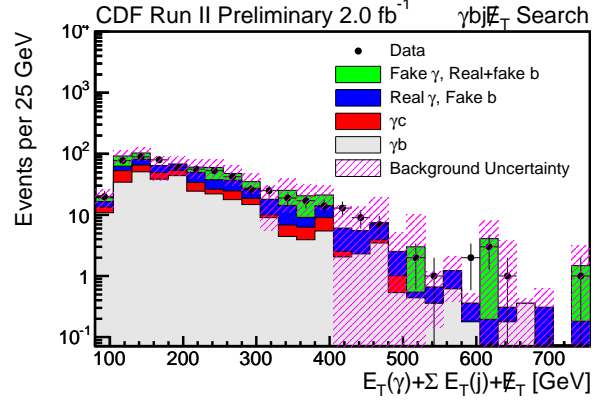
subtract the number of events containing a misidentified photon and heavy flavor from the number of events obtained from the standard photon sample fit to obtain the number of  $\gamma b$  and  $\gamma c$  events. Figure 5 shows the result of a secondary vertex fit performed on the search region using the templates to extract the fraction of  $b$ -jet and  $c$ -jet events.

The total background prediction is  $607 \pm 74 \pm 86$ , where the first uncertainty is statistical and the second systematic. The observed number of events is 617, consistent with the SM background predictions. Figure 6 shows the  $H_T$  and the number of jets distributions in the sample of a photon, a  $b$ -tagged jet, a second jet and  $\cancel{E}_T$ . This result is now published [5].

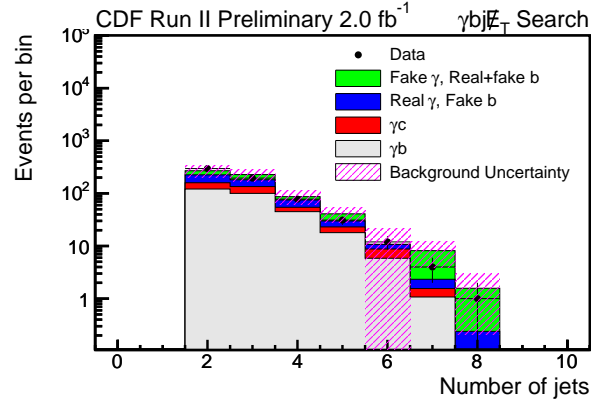
#### 4. Search for a Fermiophobic Higgs Boson in $\gamma\gamma$

The SM prediction for the Higgs,  $h \rightarrow \gamma\gamma$  branching ratio is extremely small. However, in “fermiophobic” models, where the coupling of the Higgs boson to fermions is highly suppressed, the diphoton decay can be greatly enhanced. Since for this fermiophobic case, the diphoton final state dominates at low Higgs boson masses the diphoton final state becomes the preferred search channel.

We select a diphoton sample from  $3.0 \text{ fb}^{-1}$  of data, filtered by diphoton trigger. We then require both photons to be located within central region ( $|\eta| < 1.05$ ), referred to as “central-central region”, or one photon to be in this region and the other photon in plug region ( $1.2 < |\eta| < 2.8$ ), referred to as “central-forward region”. Individual photons are required to have  $E_T > 15 \text{ GeV}$ , while the diphoton pair is required to have mass of  $m_{\gamma\gamma} > 30 \text{ GeV}/c^2$ . However, the fermiophobic Higgs boson is only produced at a non-negligible rate in association with a  $W/Z$  boson or via vector boson fusion process. Since associated



(a)



(b)

Figure 6: In (a) the  $H_T$  in the sample of a photon, a  $b$ -tagged jet, a second jet, and  $\cancel{E}_T$ . In (b) the number of jets in the sample.

production dominates the production process the optimization was performed on the basis of the associated production process alone. A selection based on the following observables was optimized: diphoton transverse momentum ( $p_T^{\gamma\gamma}$ ), transverse momentum of the second highest  $p_T$  jet ( $p_T^{j2}$ ) for hadronic decays of  $W/Z$ , and missing transverse energy ( $\cancel{E}_T$ ) or transverse momentum of an isolated track ( $p_T^{iso}$ ) for leptonic decays of  $W/Z$ . A variety of sets of these requirements which would select evidence of the  $W$  or  $Z$  boson were carried out, but the only single requirement that the diphoton transverse momentum ( $p_T^{\gamma\gamma}$ ) be greater than  $75 \text{ GeV}/c$  is approximately as sensitive as any combination of the other selection requirements. With this requirement on  $p_T^{\gamma\gamma}$ , roughly 30% of the signal remains while more than 99.5% of the background is removed.

The decay of a Higgs boson into a diphoton pair appears as a very narrow peak in the invariant mass distribution of this diphoton pair. The diphoton mass resolution determined from simulation is better than 3% for the Higgs boson mass region, as shown in

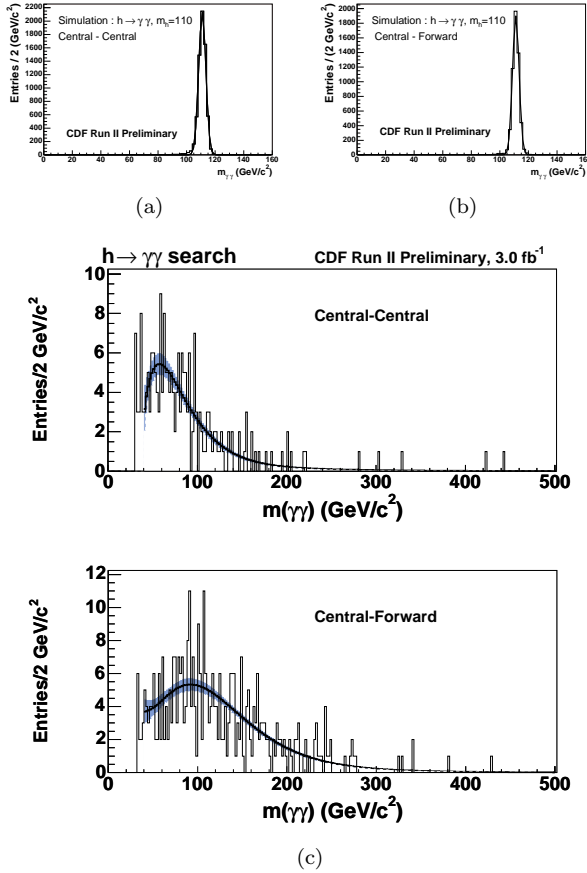


Figure 7: In (a) and (b) the expected shapes of invariant Higgs mass of the signal from simulation are shown for central-central and central-forward regions, respectively. In (c) the invariant mass distribution of central-central (top) and central-forward (bottom) photon pairs after the requirement of  $p_T^{\gamma} > 75$  GeV/c with the fit to the data for the hypothesis of a  $m_h = 100$  GeV/c<sup>2</sup>.

Fig. 7-(a) and (b). To establish the level of signal and background, we fit the diphoton mass spectrum to a background shape and the signal shape from a MC sample. The resulting invariant mass distributions of central-central and central-forward diphoton pair is shown in Fig. 7-(c).

No evidence of such a resonance appears in the data so we set the 95% C.L. upper limits both on the production cross section ( $\sigma \times B(h \rightarrow \gamma\gamma)$ ) and the branching fraction for the fermiophobic Higgs boson decay to diphotons as a function of this Higgs mass ( $m_h$ ) and exclude this type of Higgs boson mass up to 106 GeV/c<sup>2</sup>, as shown in Fig. 8. This result is now published [6]

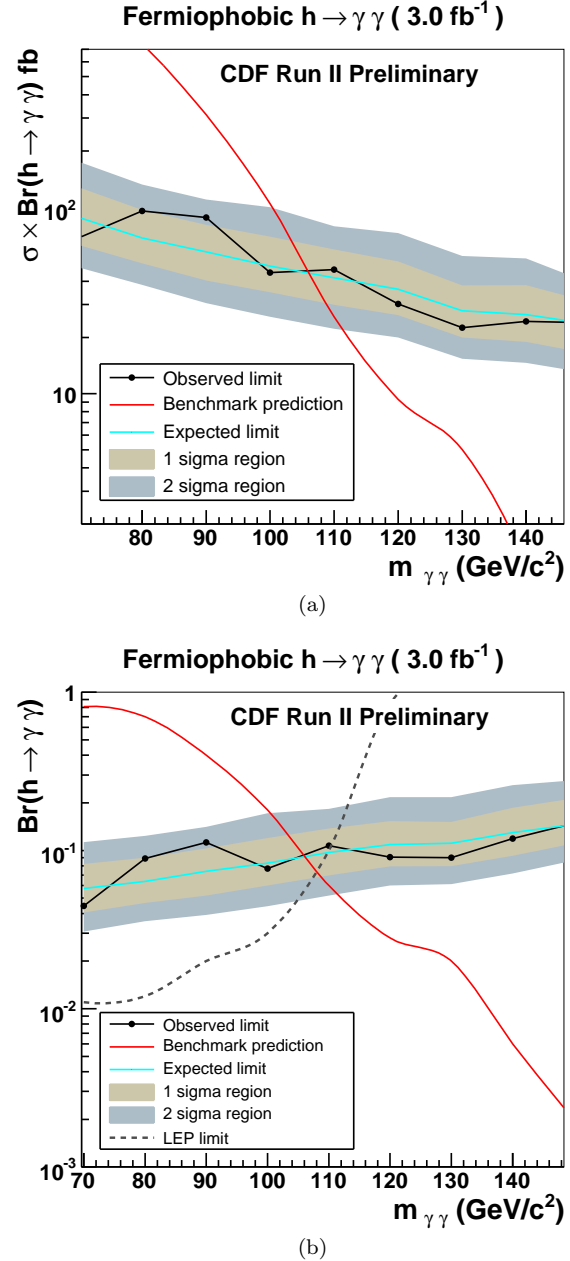


Figure 8: The 95% C.L. upper limit on the production cross section (a) and the branching fraction (b) for the fermiophobic Higgs boson decay to diphotons, as a function of  $m_h$ .

## Acknowledgments

I would like to thank the authors: R. Culbertson, H. Frisch, D. Krop, C. Pilcher, S Wilbur, S. Yu, A. Pronko, M. Goncharov, D. Toback for their analyses and help on the talk.

## References

- [1] S. Dimopoulos, S. Thomas, and J. Wells, Nucl. Phys. B **488**, 39 (1997); S. Ambrosanio, G. Kribs, and S. Martin, Phys. Rev. D **56**, 1761 (1997); G. Giudice and R. Rattazzi, Phys. Rep. **322**, 419 (1999); S. Ambrosanio, G. Kane, G. Kribs, S. Martin, and S. Mrenna, Phys. Rev. D **55**, 1372 (1997).
- [2] ALEPH Collaboration, A. Heister *et. al.*, Eur. Phys. J. C **25**, 339 (2002); A. Garcia-Bellido, Ph.D. thesis, Royal Holloway University of London (2002) (unpublished), arXiv:hep-ex/0212024.
- [3] CDF Collaboration, A. Abdulencia *et. al.*, Phys. Rev. Lett **99**, 121801 (2007); CDF Collaboration, T.Aaltonen *et. al.*, Phys. Rev. D **78**, 032015 (2008).
- [4] C.-H. Chen and J. F. Gunion, Phys. Rev. D **58**, 075005 (1998).
- [5] T. Aaltonen *et. al.*, Phys. Rev. D **80**, 052003 (2009).
- [6] T. Aaltonen *et. al.*, Phys. Rev. Lett. **103**, 061803 (2009).